



Deeply Virtual Compton Scattering on proton and neutron from deuterium with CLAS12 at Jefferson Lab

Adam HOBART, Silvia Niccolai
on behalf of the CLAS collaboration

HADRON2023
5-9 June 2023, Genova, Italy

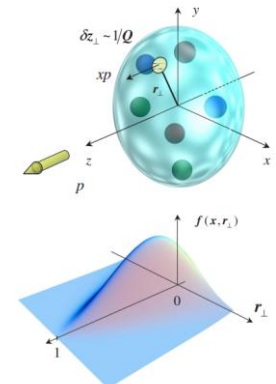




GPDs

- QCD at low energies: non perturbative regime
 - Need **structure functions** to describe nucleon structure

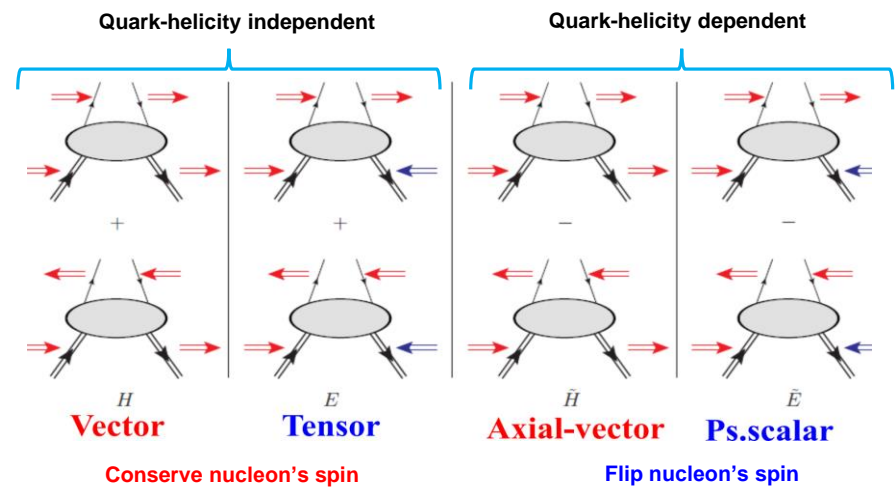
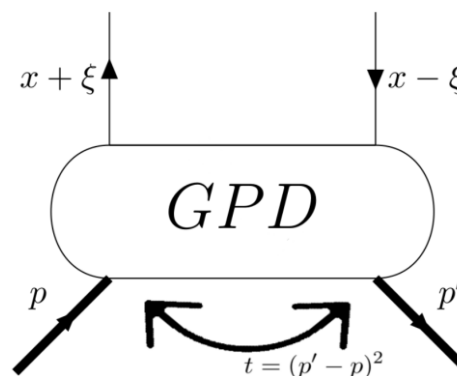
Belitsky, Radyushkin, Physics Reports, 2005



GPDs

Correlation of transverse position and longitudinal momentum of partons in the nucleon
& the spin structure - through Ji's sum rule X. Ji, Phy.Rev.Lett.78,610(1997)

- GPDs can be accessed through **exclusive lepton production reactions**
- At leading order QCD, chiral-even (quark helicity is conserved), quark sector: **4 GPDs** for each quark flavor H, \tilde{H}, E and \tilde{E}
- GPDs depend on x, ξ and $t = (p' - p)^2$





Why are GPDs important?

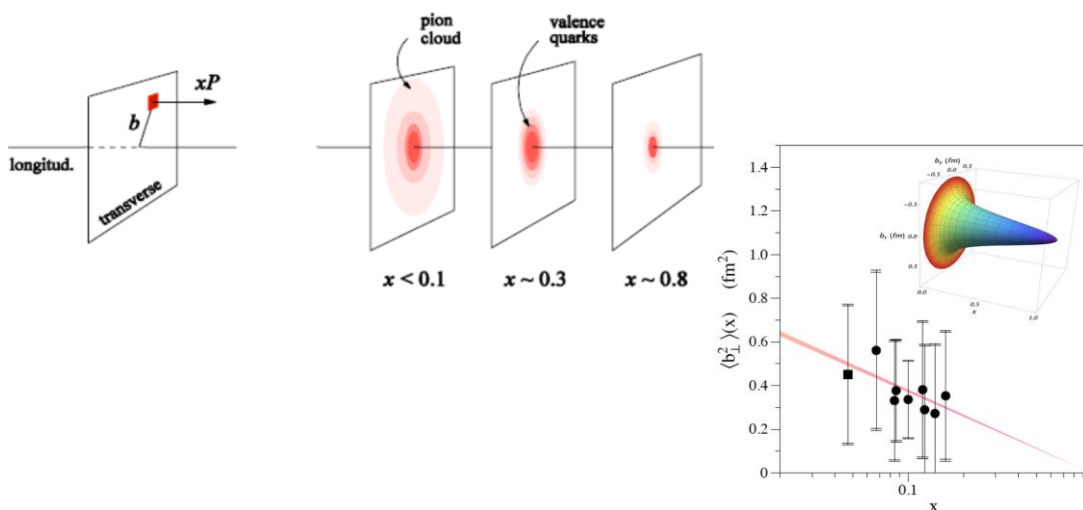
- GPDs: Fourier transforms of non-local, non-diagonal QCD operators

Nucleon tomography

M. Burkardt, PRD 62, 71503 (2000)

$$q(x, b_\perp) = \int_0^\infty \frac{d^2 \Delta_\perp}{(2\pi)^2} e^{i \Delta_\perp b_\perp} H(x, 0, -\Delta_\perp^2)$$

$$\Delta q(x, b_\perp) = \int_0^\infty \frac{d^2 \Delta_\perp}{(2\pi)^2} e^{i \Delta_\perp b_\perp} \tilde{H}(x, 0, -\Delta_\perp^2)$$



R. Dupré, M. Guidal, M. Vanderhaeghen, PRD95, 011501 (2017)

Quark angular momentum

X. Ji, Phys.Rev.Lett.78,610(1997)

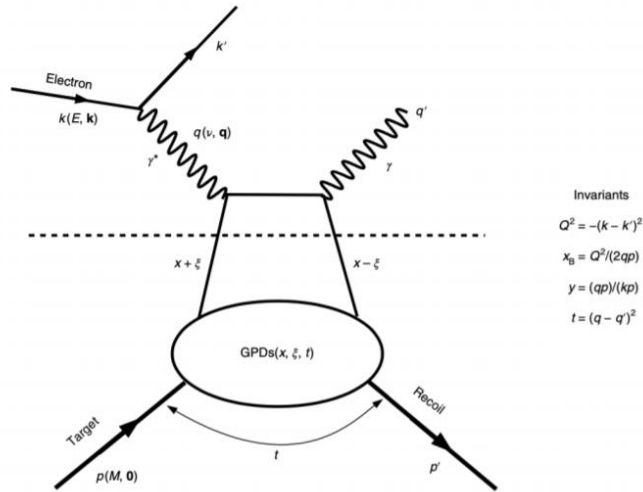
$$\frac{1}{2} \int_{-1}^1 x dx (H(x, \xi, t=0) + E(x, \xi, t=0)) = J = \frac{1}{2} \Delta \Sigma + \Delta L$$

$$\text{Nucleon spin: } \frac{1}{2} = \frac{1}{2} \Delta \Sigma + \Delta L + \Delta G$$

- The **intrinsic spin of the quarks** can not explain the origin of the **spin of the nucleon (nucleon Spin Crisis)**
- Intrinsic spin of the gluons**
- GPDs:** quantify the contribution of **orbital angular momentum** of quarks to the nucleon spin



Deeply Virtual Compton Scattering of leptons off nucleons



- DVCS allows access to 4 complex GPDs-related quantities:
 - Compton Form Factors (x, ξ, t) (CFFs)

$$\mathcal{H} = \sum_q e_q^2 \left\{ i \pi [H^q(\xi, \xi, t) - H^q(-\xi, \xi, t)] + \mathcal{P} \int_{-1}^1 dx H^q(x, \xi, t) \left[\frac{1}{\xi-x} - \frac{1}{\xi+x} \right] \right\}$$

- x can not be accessed experimentally by DVCS:
Models needed to map the x dependence

$$\sigma(eN \rightarrow eN\gamma) = \left| \text{DVCS} + \text{Bethe-Heitler (BH)} \right|^2$$

BH is purely electromagnetic and parametrised by FFs

- Experimentally measured observables:
 - Sensitive to the DVCS-BH interference part (linear in CFFs)
 - Should have: Beam polarized and/or target polarized
 - Access to a combinations of CFFs
 - The separation of CFFs requires the measurement of several observables
 - Depending on the target (proton or neutron): different sensitivity to the CFFs (GPDs)
 - The flavor separation of GPDs requires measurements on both nucleons

$$(H, E)_u(\xi, \xi, t) = \frac{9}{15} [4(H, E)_p(\xi, \xi, t) - (H, E)_n(\xi, \xi, t)]$$

$$(H, E)_d(\xi, \xi, t) = \frac{9}{15} [4(H, E)_n(\xi, \xi, t) - (H, E)_p(\xi, \xi, t)]$$



Deeply Virtual Compton Scattering: physics observables and their link to CFFs

Different contributions from F_1 and F_2 for the different nucleons

Polarized beam, unpolarized target

$$\Delta\sigma_{LU} \sim \sin(\phi) \Im\{F_1 \mathbf{H} + \xi(F_1 + F_2) \tilde{\mathbf{H}} - k F_2 \mathbf{E} + \dots\}$$

Unpolarized beam, polarized target

$$\Delta\sigma_{UL} \sim \sin(\phi) \Im\left\{F_1 \tilde{\mathbf{H}} + \xi(F_1 + F_2) \left(\mathbf{H} + \frac{x_b}{2} \mathbf{E}\right) - \xi k F_2 \tilde{\mathbf{E}}\right\}$$

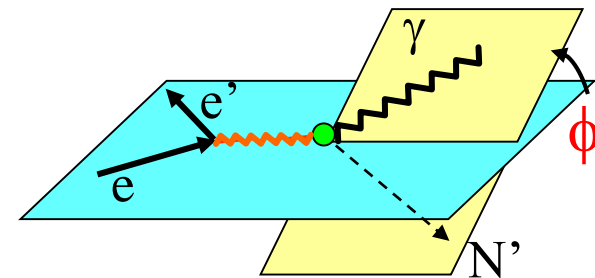
polarized beam, longitudinal polarized target

$$\Delta\sigma_{LL} \sim (A + B \cos(\phi)) \Re\{F_1 \tilde{\mathbf{H}} + \xi(F_1 + F_2) \left(\mathbf{H} + \frac{x_b}{2} \mathbf{E}\right) + \dots\}$$

unpolarized beam, transverse polarized target

$$\Delta\sigma_{UT} \sim \cos(\phi) \sin(\phi_s - \phi) \Im\{k(F_2 \mathbf{H} - F_1 \mathbf{E}) + \dots\}$$

Observable	Proton	Neutron
$\Delta\sigma_{LU}$	$\Im\{\mathbf{H}_p, \tilde{\mathbf{H}}_p, E_p\}$	$\Im\{H_n, \tilde{H}_n, \mathbf{E}_n\}$
$\Delta\sigma_{UL}$	$\Im\{\mathbf{H}_p, \tilde{\mathbf{H}}_p\}$	$\Im\{\mathbf{H}_n, E_n\}$
$\Delta\sigma_{LL}$	$\Re\{\mathbf{H}_p, \tilde{\mathbf{H}}_p\}$	$\Re\{\mathbf{H}_n, E_n\}$
$\Delta\sigma_{UT}$	$\Im\{\mathbf{H}_p, \mathbf{E}_p\}$	$\Im\{\mathbf{H}_n\}$



- DVCS with an unpolarized deuterium target :

- Scattering off neutron (nDVCS): GPD **E**

- Determination of Ji sum rule
 - Contribution of orbital angular momentum of quarks to the nucleon spin

$$\frac{1}{2} \int_{-1}^1 x dx (H(x, \xi, t=0) + E(x, \xi, t=0)) = J = \frac{1}{2} \Delta \Sigma + \Delta L$$

- Scattering off proton (pDVCS): GPD **H**

- Quantify medium effects
 - Essential for the extraction of BSA of a “free” neutron (deconvoluting medium effect via comparison with DVCS on hydrogen target)

- The BSA for nDVCS:

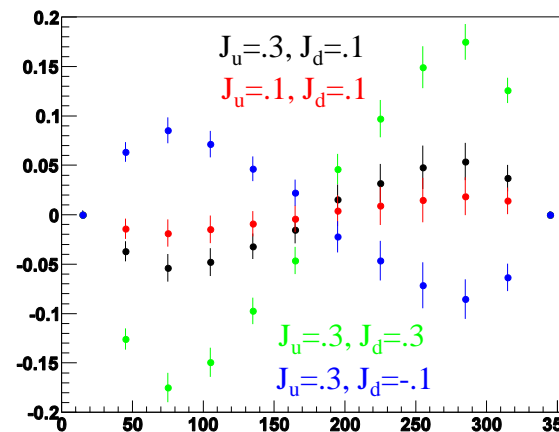
- is complementary to the TSA for pDVCS on transverse target, aiming at E
- depends strongly on the kinematics → wide coverage needed
- is smaller than for pDVCS → more beam time needed to achieve reasonable statistics

Different contributions from F_1 and F_2 for the different nucleons

Observable	Proton	Neutron
$\Delta\sigma_{LU}$	$\Im\{\mathbf{H}_p, \tilde{\mathbf{H}}_p, E_p\}$	$\Im\{H_n, \tilde{H}_n, E_n\}$
$\Delta\sigma_{UL}$	$\Im\{\mathbf{H}_p, \tilde{\mathbf{H}}_p\}$	$\Im\{\mathbf{H}_n, E_n\}$
$\Delta\sigma_{LL}$	$\Re\{\mathbf{H}_p, \tilde{\mathbf{H}}_p\}$	$\Re\{\mathbf{H}_n, E_n\}$
$\Delta\sigma_{UT}$	$\Im\{\mathbf{H}_p, E_p\}$	$\Im\{\mathbf{H}_n\}$

Model predictions (VGG) for different values
of quarks' angular momentum

Phys. Rev. D **60**, 094017

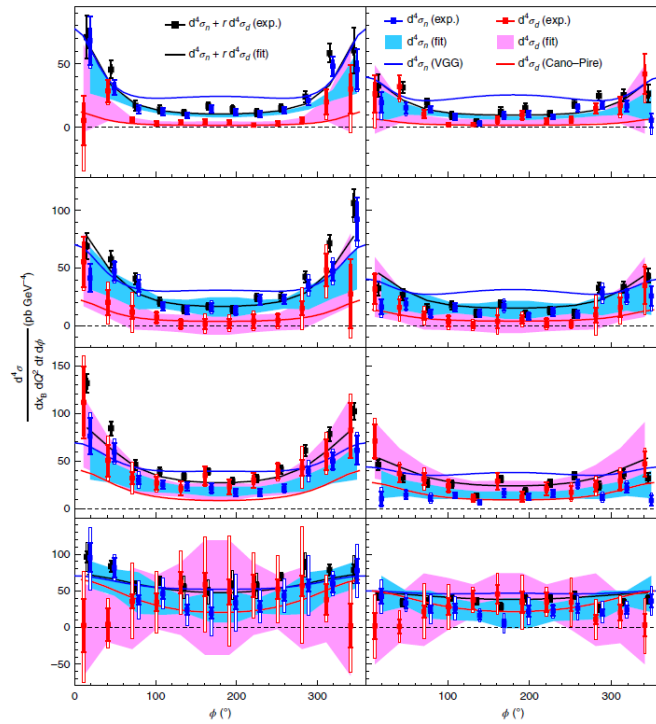




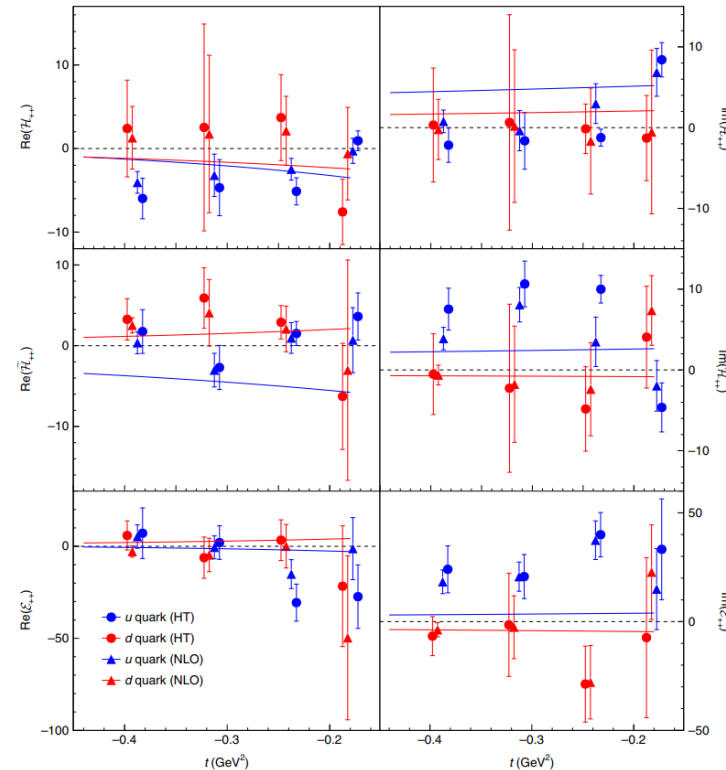
Deeply Virtual Compton Scattering with an unpolarized deuterium target

- Previous pioneering measurement of nDVCS (Jlab Hall A @ 6 GeV)
 - Beam-energy « Rosenbluth » separation of nDVCS CS using an LD2 target and two different beam energies
 - First observation of non-zero nDVCS CS
- No neutron detection $D(e, e'\gamma)X - H(e, e'\gamma)X = n(e, e'\gamma)n + d(e, e'\gamma)d + \dots$

One measured kinematical point:
 $Q^2=1.9 \text{ GeV}^2$ and $x_B=0.36$



+data from: Mazouz, M. et al. Phys. Rev. Lett. 99, 242501 (2007).



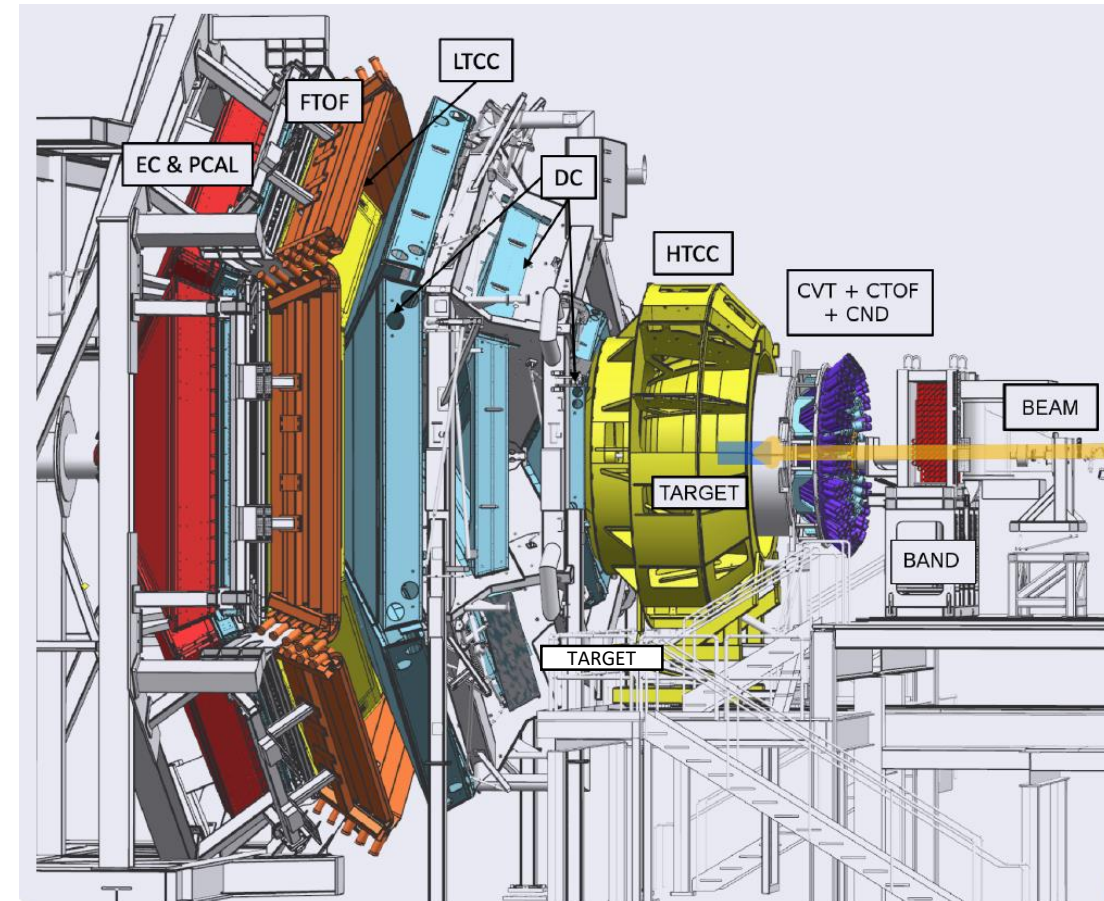
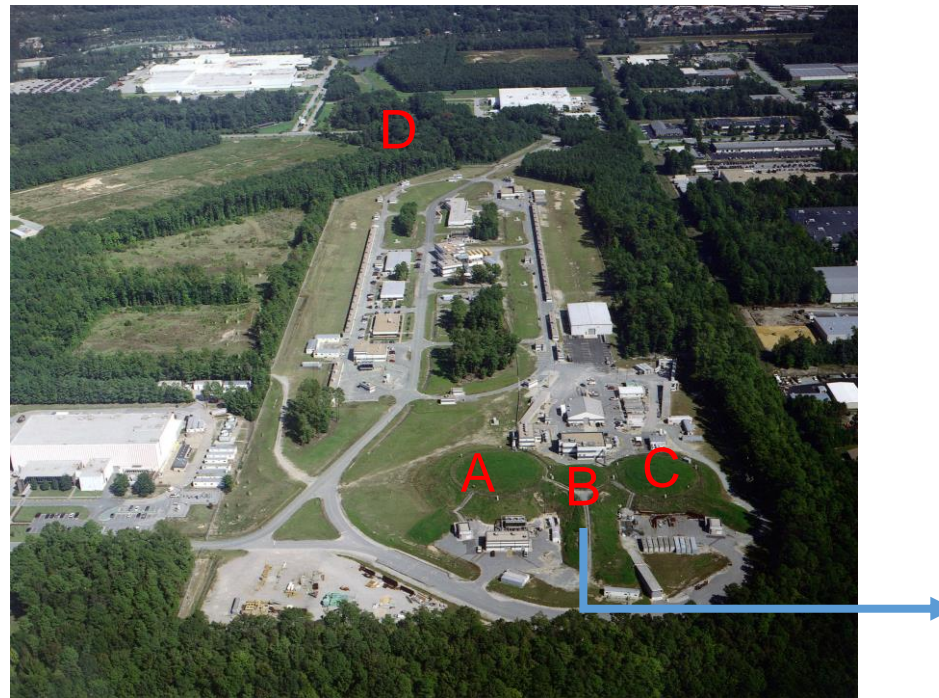
Benali, M., Desnault, C., Mazouz, M. et al. Nat. Phys. 16, 191–198 (2020)



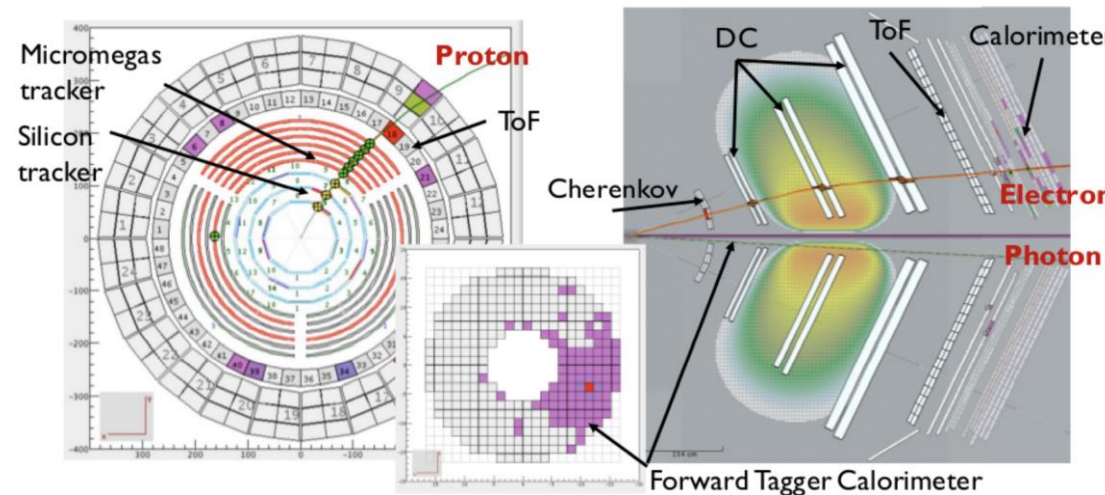
The CEBAF and CLAS12 at Jefferson Laboratory

Continuos Electron Beam Accelerator Facility

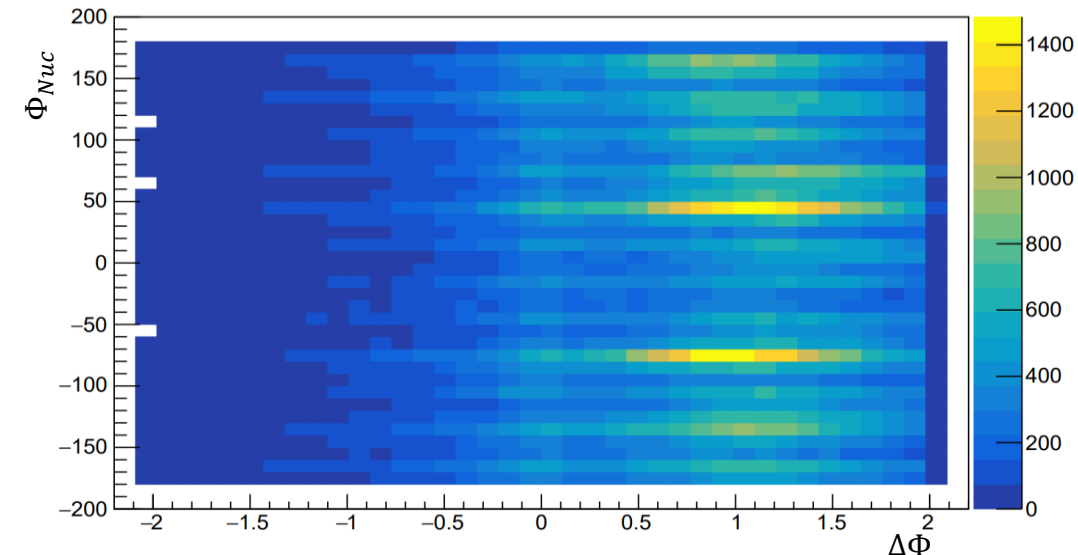
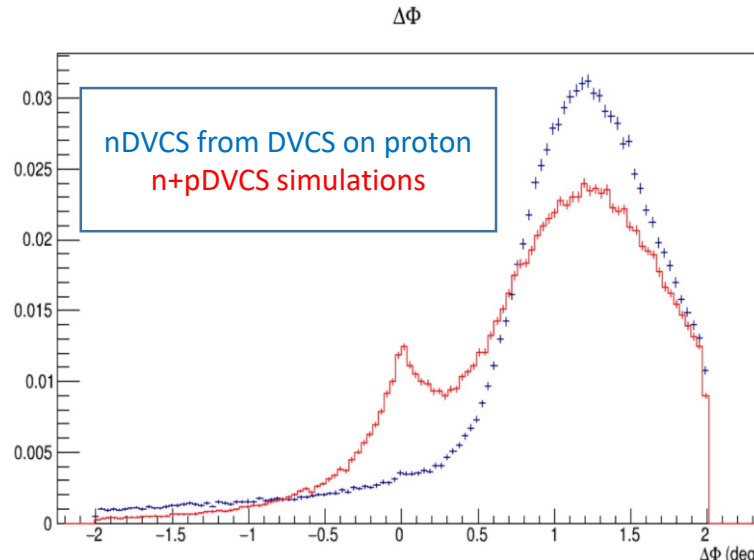
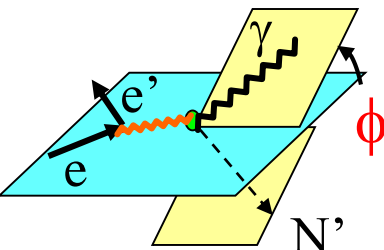
- Up to 12 GeV electrons
- Two anti-parallel linacs, with recirculating arcs on both ends
- 4 experimental halls



- A 10.6/10.4/10.2 GeV electron beam
 - With an average polarization of 86%
 - Scattering off an unpolarized Liquid Deuterium target of 5 cm length
- The exclusivity of the event is ensured by:
 - Electron detection: Cerenkov detector, drift chambers and electromagnetic calorimeter
 - Photon detection: sampling calorimeter or a small PbWO₄-calorimeter close to the beamline
 - Proton detection: Silicon and Micromegas detector OR Neutron detection: Central Neutron Detector
- For Neutron Detection:
 - Machine Learning techniques are applied to improve the Identification and reduce charged particle contamination



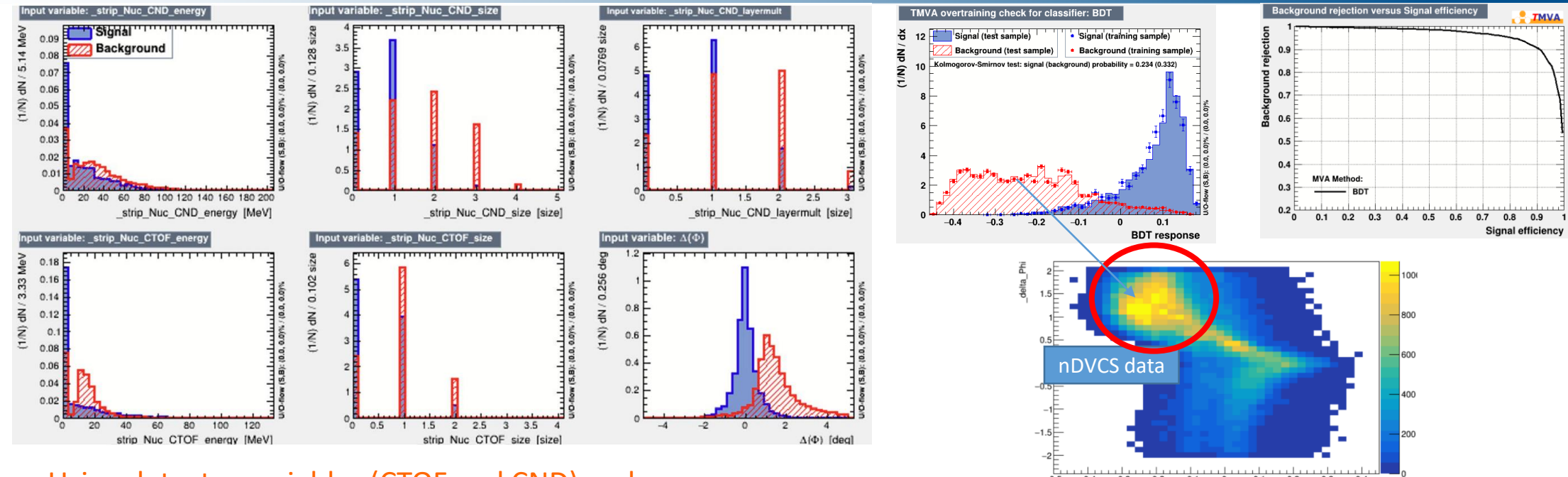
- The tracking of the CVT is neither 100% efficient nor uniform
- In the dead regions of the CVT **protons** have no associated track and thus can be **misidentified as neutrons**
- Protons roughly account for more than **>40% contamination in the “nDVCS” signal sample**
- Current approach, based on Machine Learning & Multi-Variate Algorithms:
 - We reconstruct nDVCS from DVCS experiment on proton requiring neutron PID : **selected neutron are misidentified protons**
 - We use this sample to determine the characteristics of fake neutrons in low- and high-level reconstructed variables
 - Based on those characteristics we subtract the fake neutrons contamination from nDVCS
 - As a « signal » sample in the training of the ML we use $ep \rightarrow ep\pi^+$ events from DVCS experiment on proton



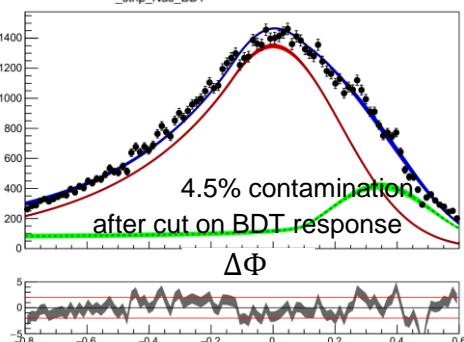
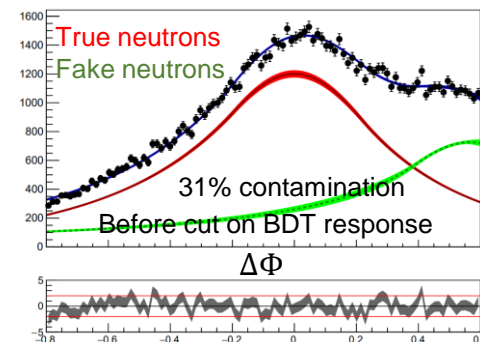


Improving the neutron selection with ML techniques

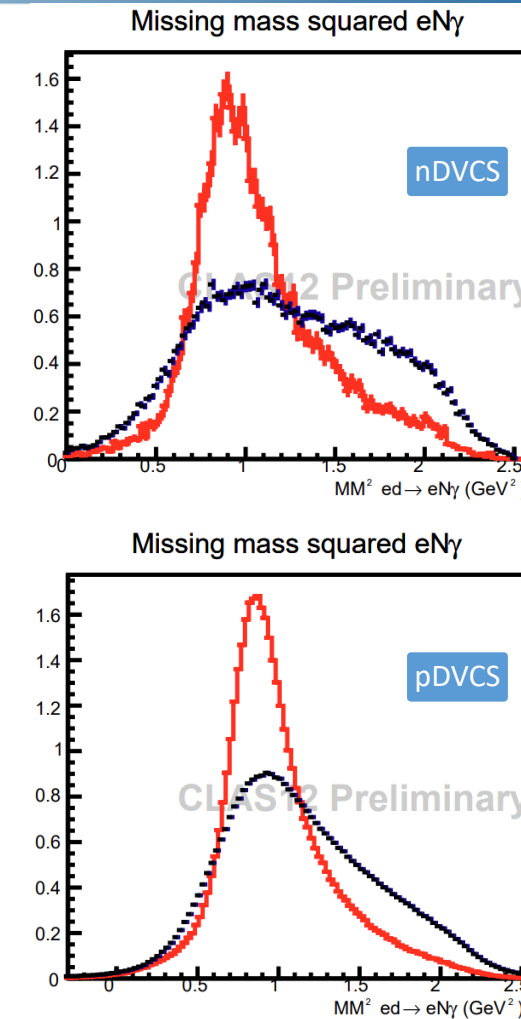
Under internal review



- Using detector variables (CTOF and CND) and one exclusivity variable ($\Delta\Phi$)
- Directly trained on data
- Better optimization of signal to background ratio than straight cuts
- Few percent irreducible contamination is to be taken as a systematic on the BSA



- The nDVCS (pDVCS) final state is selected with the following exclusivity criteria: (N:nucleon)
 - Missing mass
 - $e d \rightarrow e N \gamma X$
 - $e N \rightarrow e N \gamma X$
 - $e N \rightarrow e N X$
 - Missing momentum
 - $e d \rightarrow e N \gamma X$
 - $\Delta\Phi, \Delta t, \theta(\gamma, X)$
 - Difference between two ways of calculating Φ and t
 - Cone angle between measured and reconstructed photon
- Exclusivity selection is optimized with a 4-D χ^2 -like distribution including $\Delta\Phi, \Delta t, \theta(\gamma, X)$ and missing mass $e N \rightarrow e N X$



π^0 background contamination is estimated using simulations

- Subtraction using simulations of the background channel
 - Monte Carlo simulations:
 - GPD-based event generator for DVCS/pi0 on deuterium
 - DVCS amplitude calculated according to the BKM formalism
 - Fermi-motion distribution evaluated according to Paris potential
- Estimate the ratio of partially reconstructed eN π^0 (1 photon) decay to fully reconstructed eN π^0 decays in MC
 - This is done for each kinematic bin to minimize MC model dependence

- Multiply this ratio by the number of reconstructed eN π^0 in data to get the number of eN π^0 (1 photon) in data
- Subtract this number from DVCS reconstructed decays in data per each kinematical bin

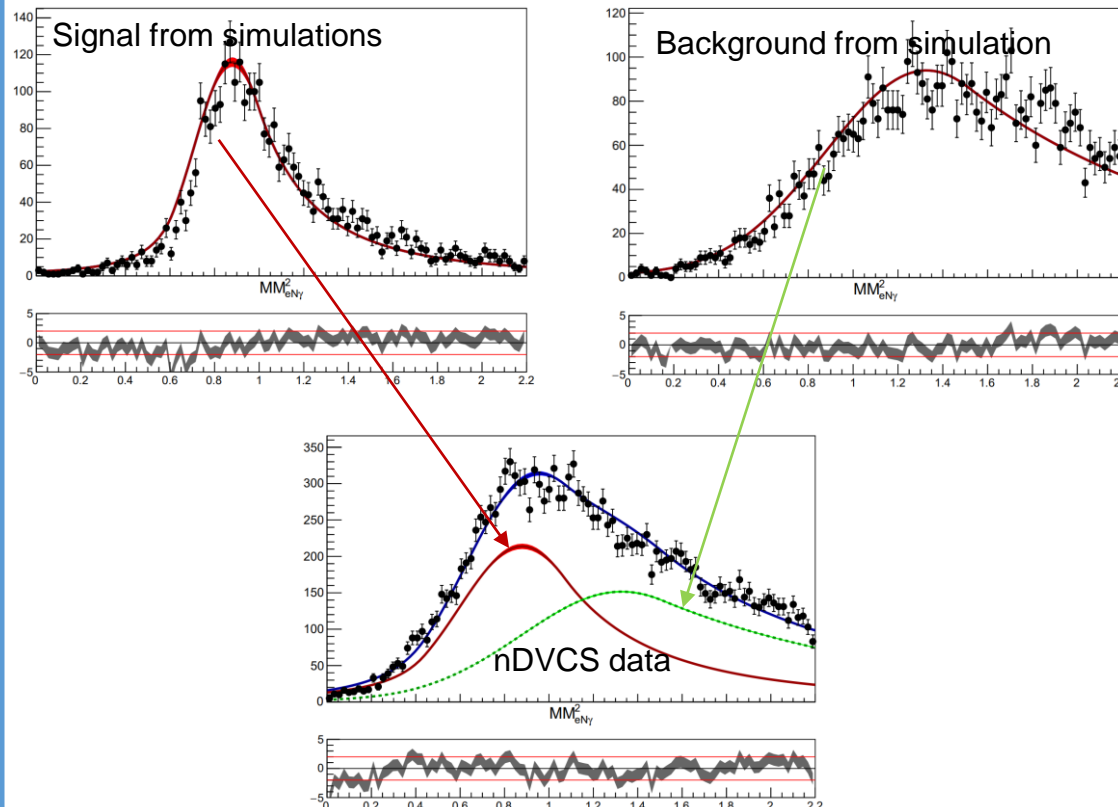
$$\text{Simulations: } R = \frac{N(eN\pi_{1\gamma}^0)}{N(eN\pi^0)}$$

$$\text{Data: } N(eN\pi_{1\gamma}^0) = R * N(eN\pi^0)$$

$$N(\text{DVCS}) = N(\text{DVCS}_{\text{recon}}) - N(eN\pi_{1\gamma}^0)$$

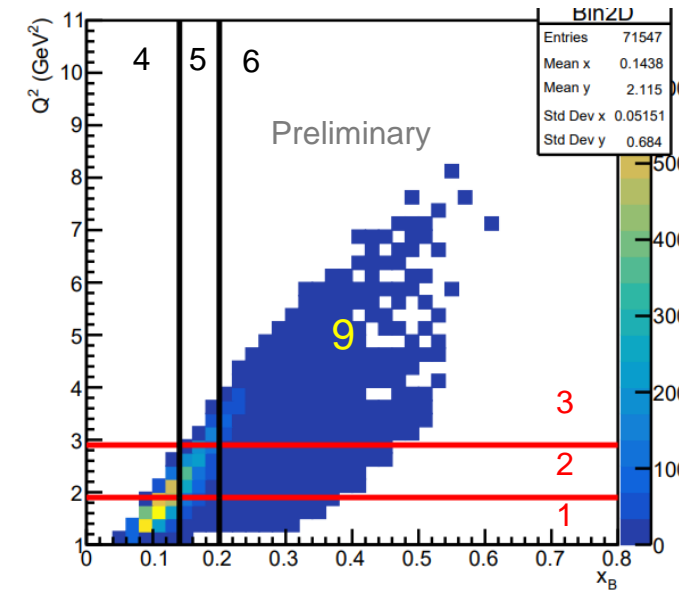
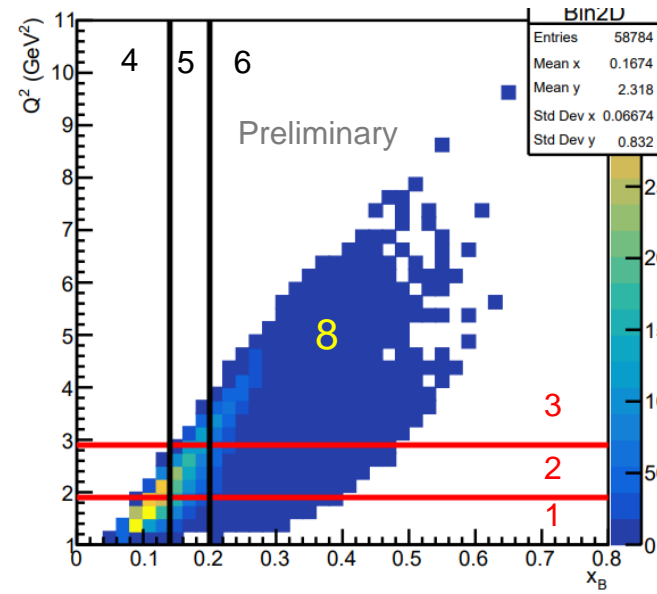
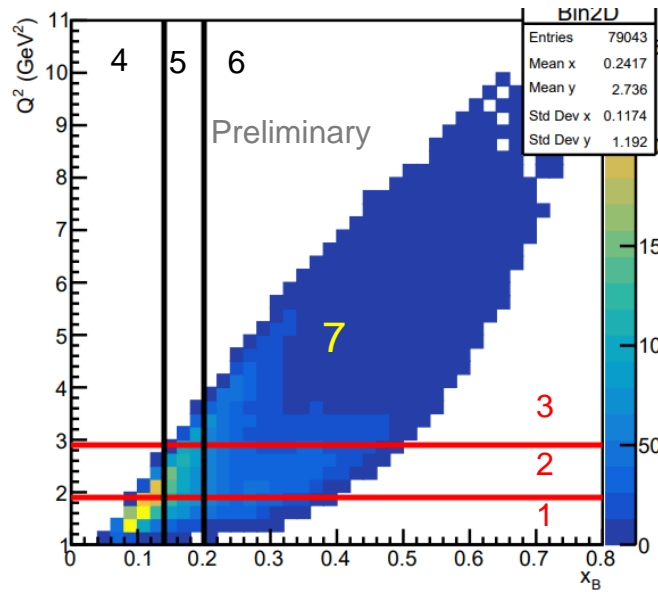
- π^0 background subtraction is also performed by statistical unfolding of contribution to the missing mass spectrum

M. Pivk and F.R. Le Diberder, NIMA 555 1 2005



The difference between the estimations of background from both methods is considered as a systematic

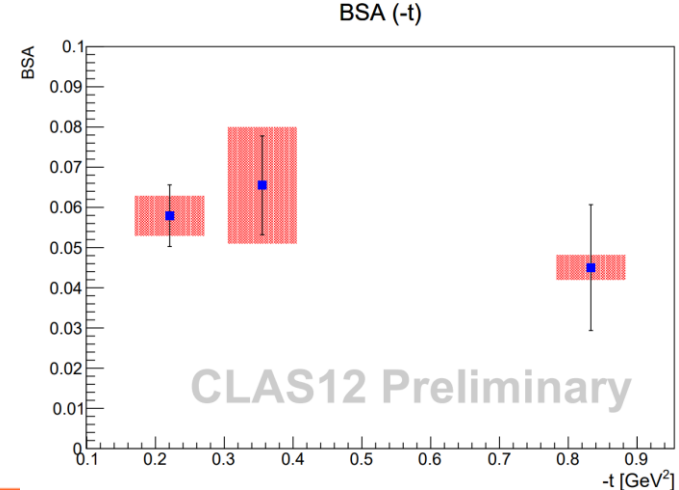
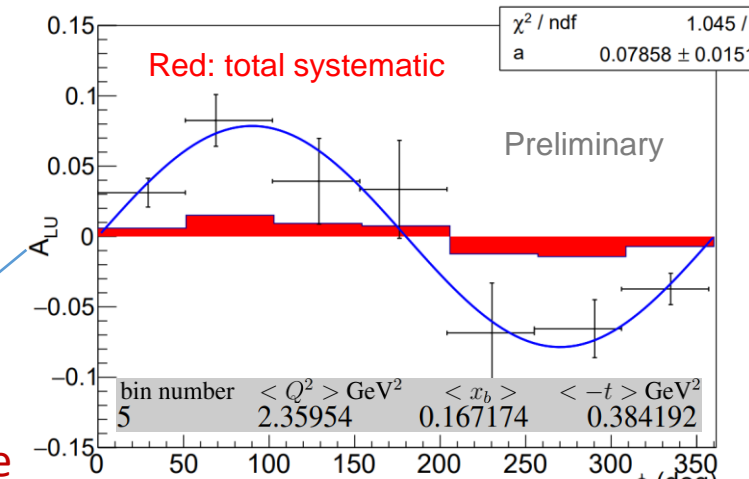
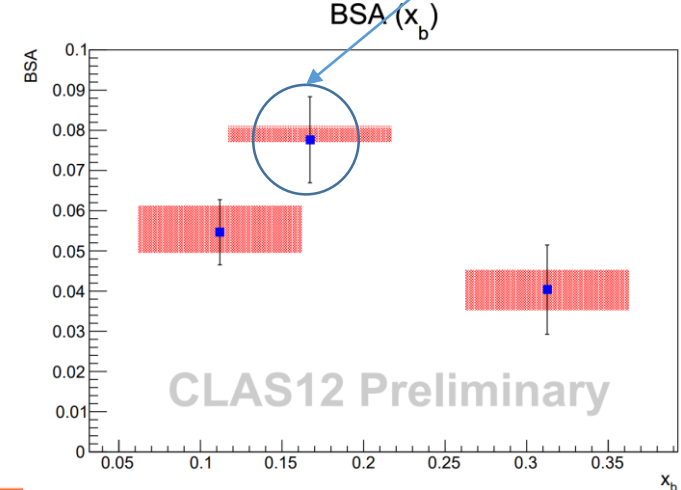
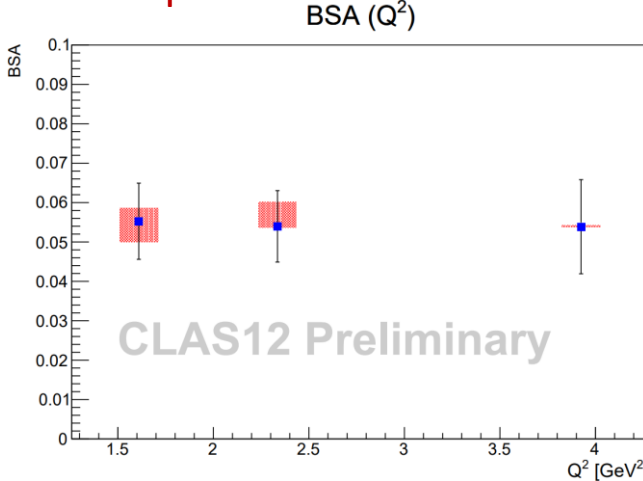
First-time measurement of nDVCS with detection of the active neutron



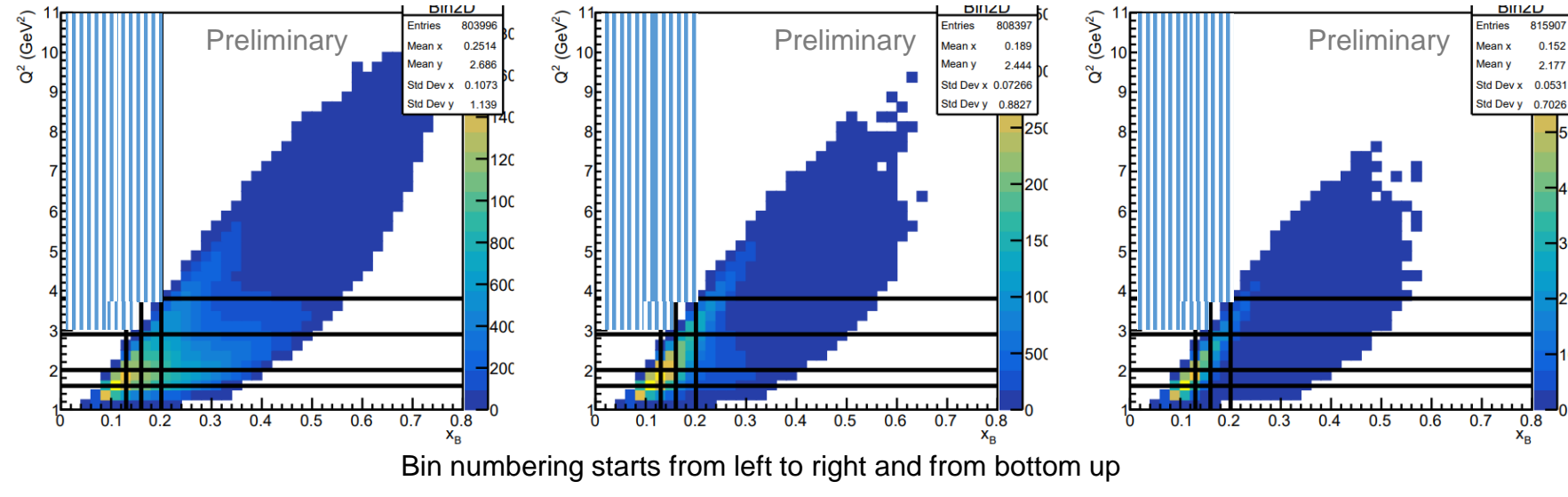
- Compared to the previous experiment, CLAS12 provides :
 - The possibility to scan the BSA of nDVCS on a wide phase space
 - The possibility to reach the high Q^2 high x_b region of the phase space
 - Exclusive measurement with the detection of the active neutron
- Hall A @ CLAS: one measured kinematical point at $Q^2=1.9$ GeV^2 and $x_B=0.36$

bin number	$\langle Q^2 \rangle \text{ GeV}^2$	$\langle x_b \rangle$	$\langle -t \rangle \text{ GeV}^2$
1	1.60973	0.132015	0.388061
2	2.33568	0.199322	0.467386
3	3.92472	0.314797	0.667296
4	1.70901	0.111932	0.324567
5	2.35954	0.167174	0.384192
6	3.29066	0.312552	0.70405
7	2.91918	0.277885	0.832902
8	2.44265	0.185242	0.355265
9	2.16854	0.149355	0.22063

- Observation of positive BSA for nDVCS
- Systematic errors include:
 - Error due to beam polarization
 - Error due to selection cuts
 - Error due to residual proton contamination
 - Error due to merging of data sets with different energies
 - Error due to π^0 background subtraction
- Statistics is expected to double with remaining scheduled beam time and improvements of the reconstruction software

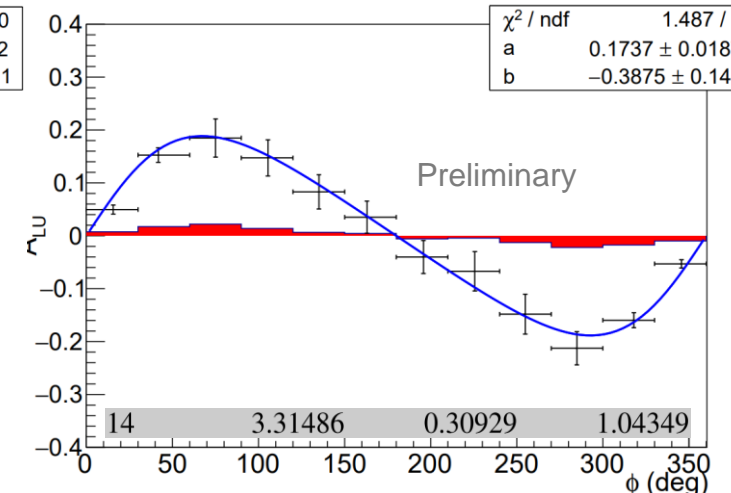
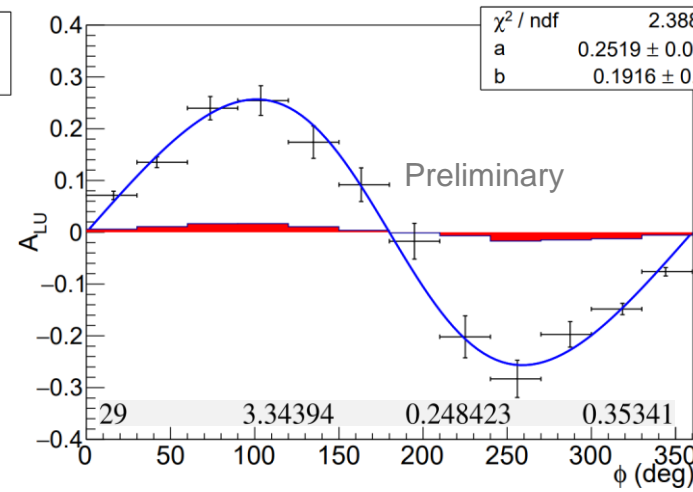
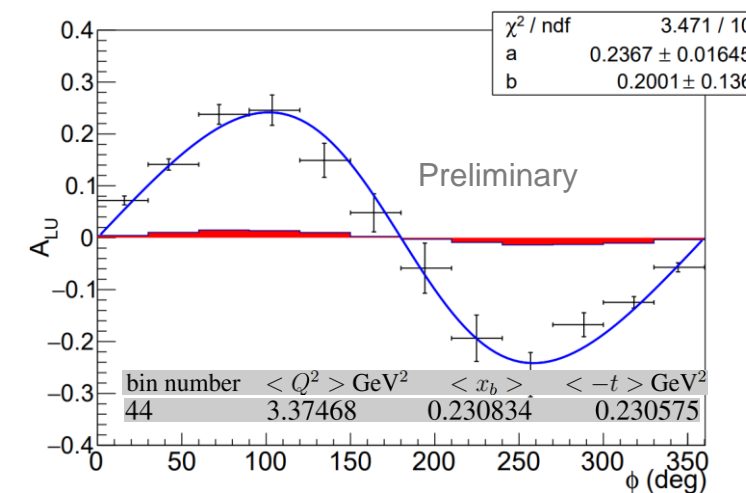
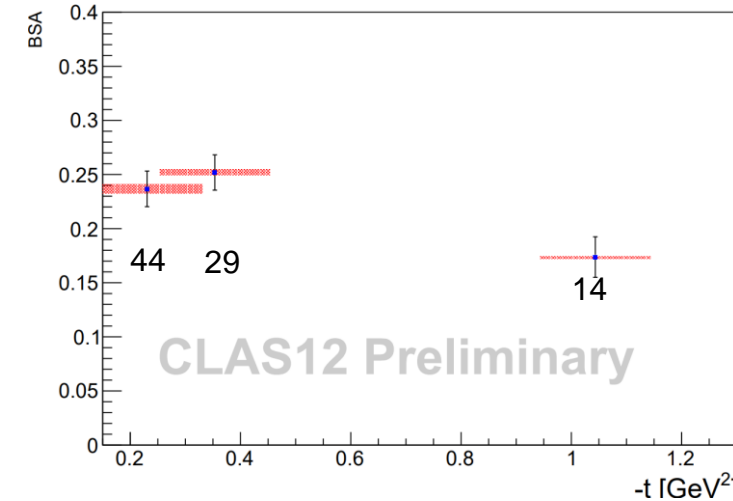


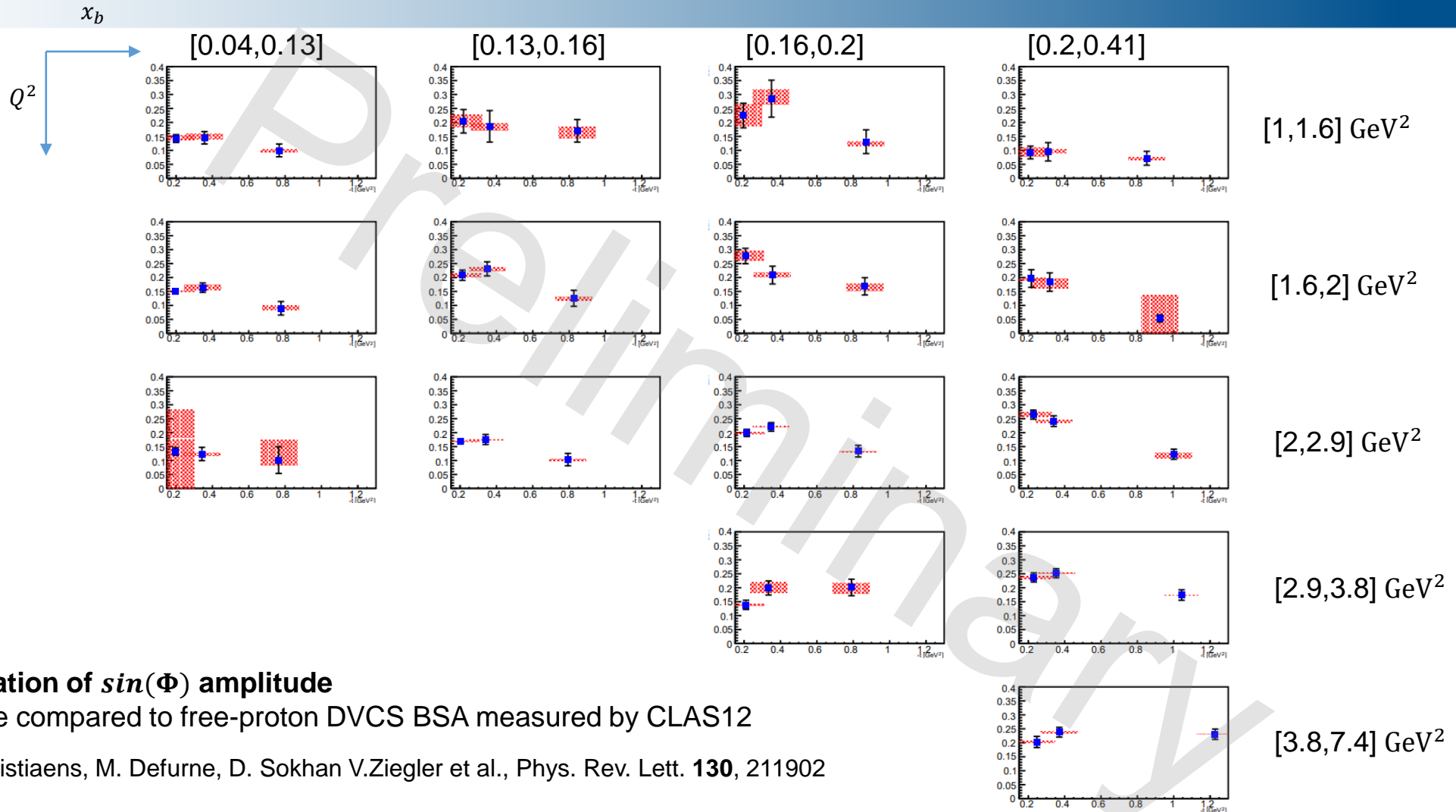
First-time measurement of incoherent pDVCS on deuteron



- Complementary to previous experiment on proton target:
 - Quantify medium effects on GPDs

- Systematic errors include:
 - Error due to beam polarization
 - Error due to selection cuts
 - Error due to merging of data sets with different energies
 - Error due to π^0 background subtraction
- Statistics is expected to triple with remaining scheduled beam time and improvements of the reconstruction software





Variation of $\sin(\Phi)$ amplitude

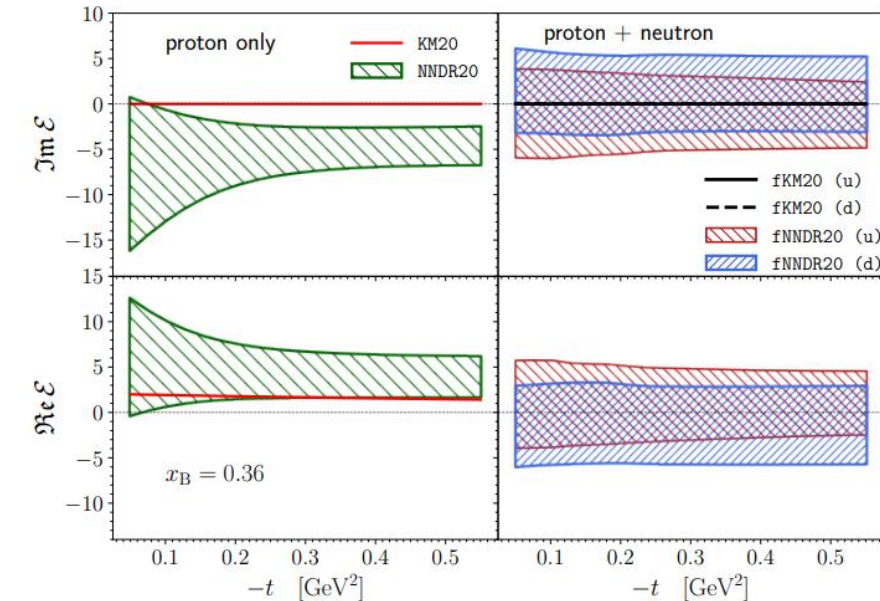
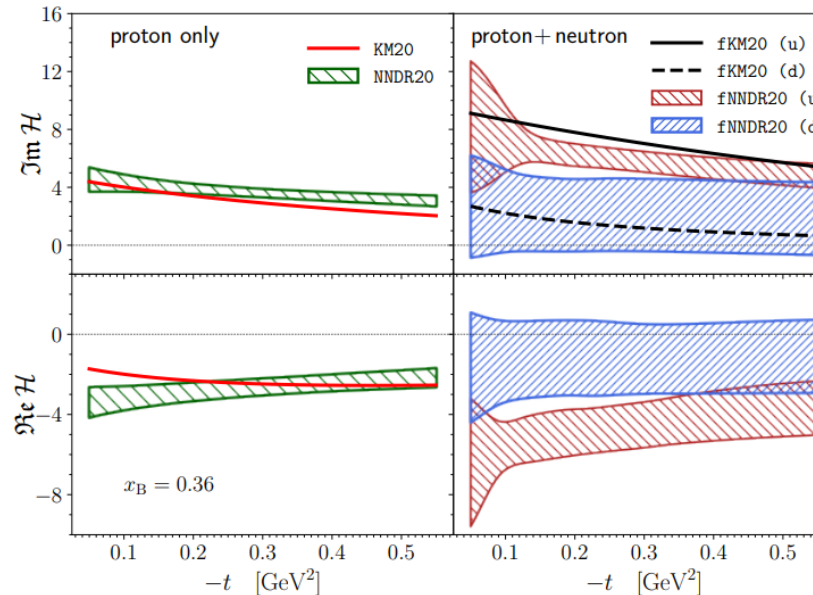
To be compared to free-proton DVCS BSA measured by CLAS12

G. Christiaens, M. Defurne, D. Sokhan V.Ziegler et al., Phys. Rev. Lett. **130**, 211902



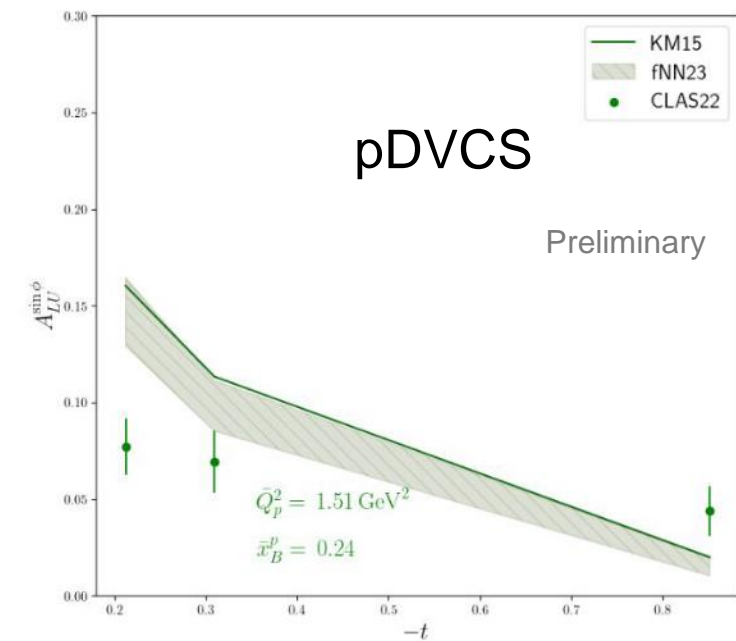
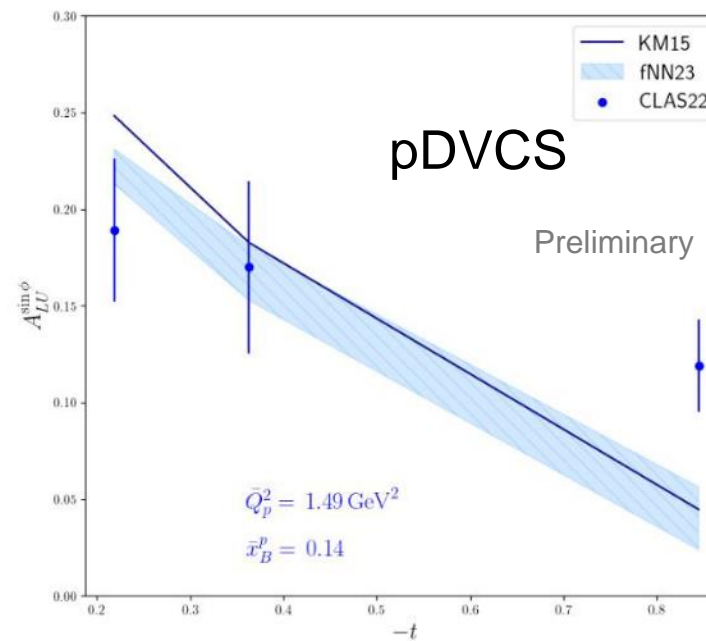
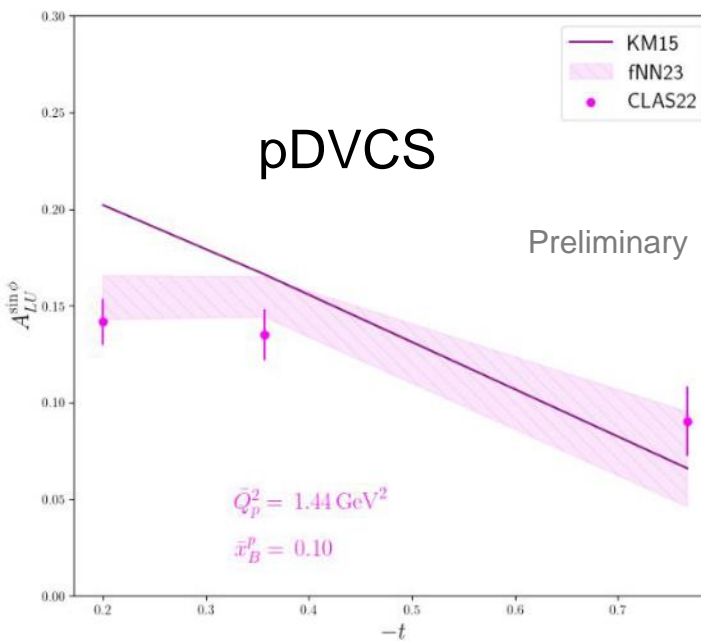
Impact of new data

- Previous attempt at flavor separation by Marija Čuić and Krešimir Kumerički arxiv 2007.00029
- Data from CLAS6 and Hall A at JLab

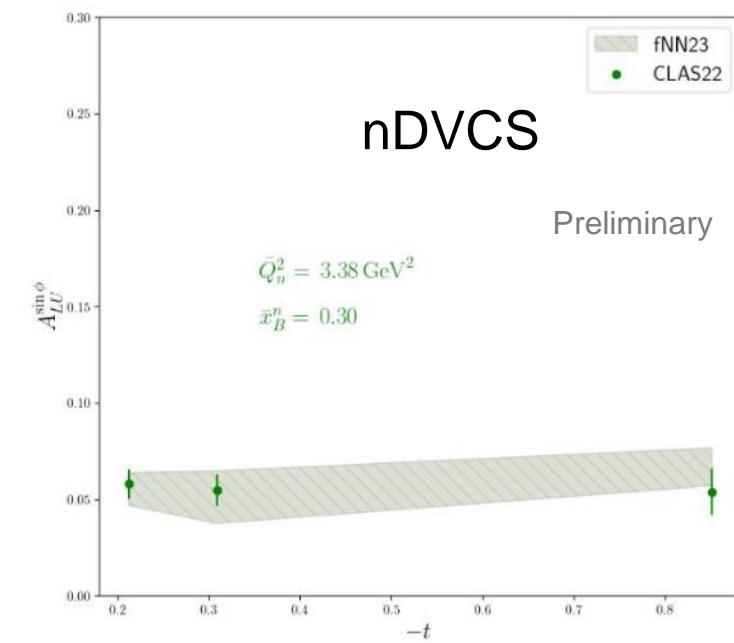
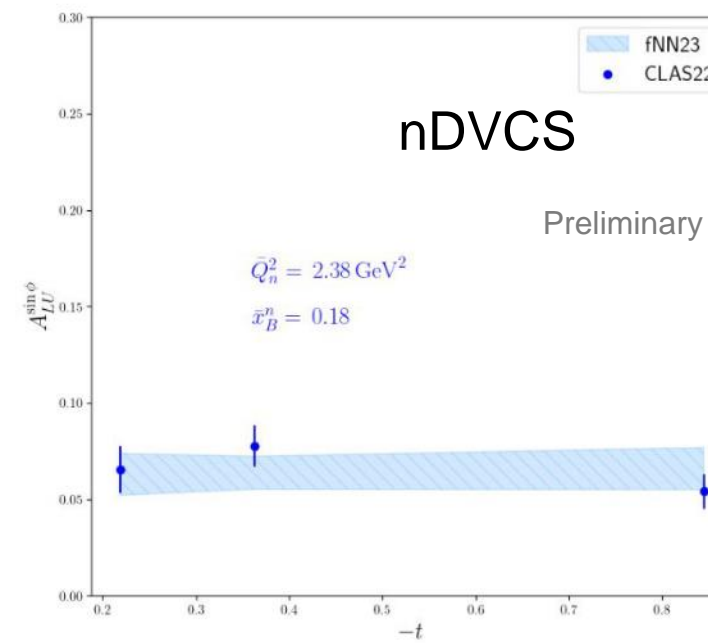
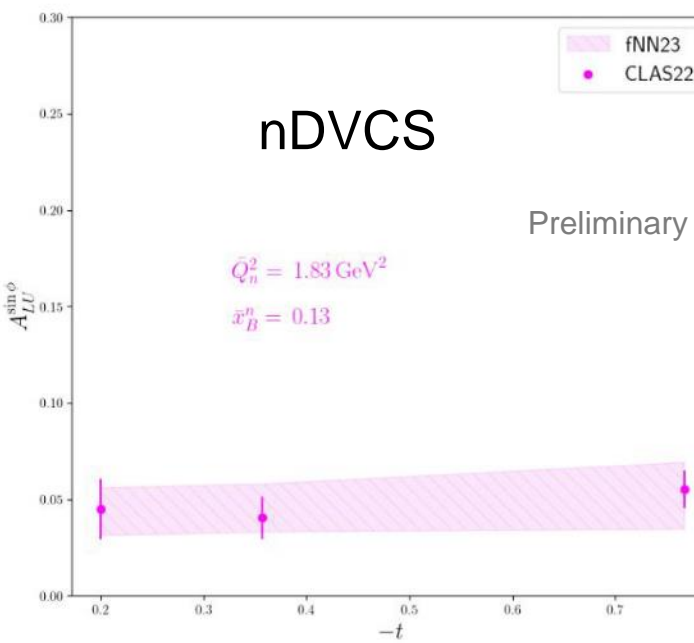


- up and down contributions to CFF H cleanly separated
- CFF E cannot be separated

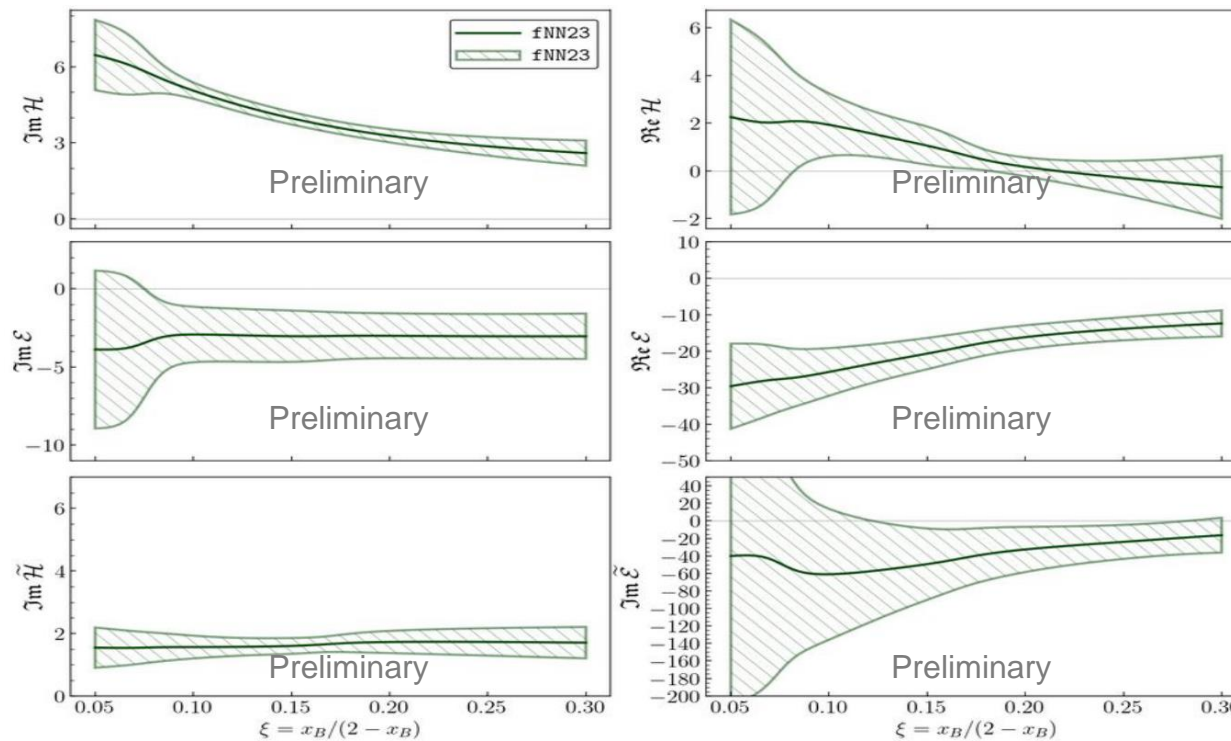
- Testing previously trained NN fits on new data was not appropriate
 - Reweighting procedure where only subset of neural nets that describes the new data well is kept in the model did not succeed
 - New data falls outside of the kinematics region of the trained models
- Solution: train new models with old CLAS6 and new CLAS12 data included in the training



- Testing previously trained NN fits on new data was not appropriate
 - Reweighting procedure where only subset of neural nets that describes the new data well is kept in the model did not succeed
 - New data falls outside of the kinematics region of the trained models
- Solution: train new models with old CLAS6 and new CLAS12 data included in the training

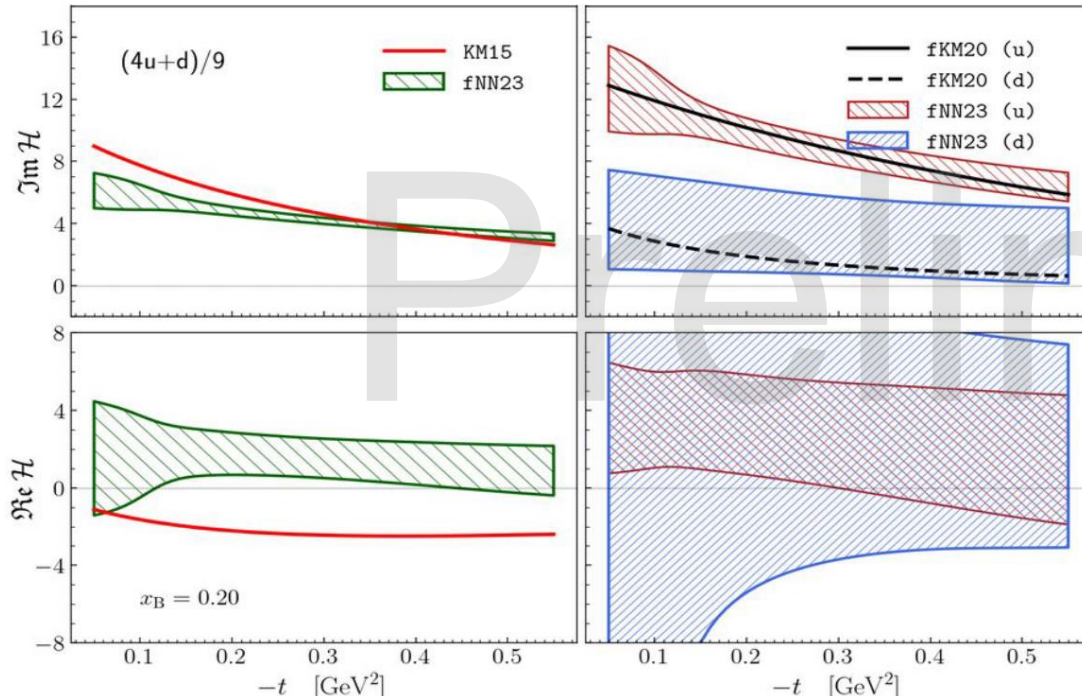


- Extraction of 6 out of 8 CFFs

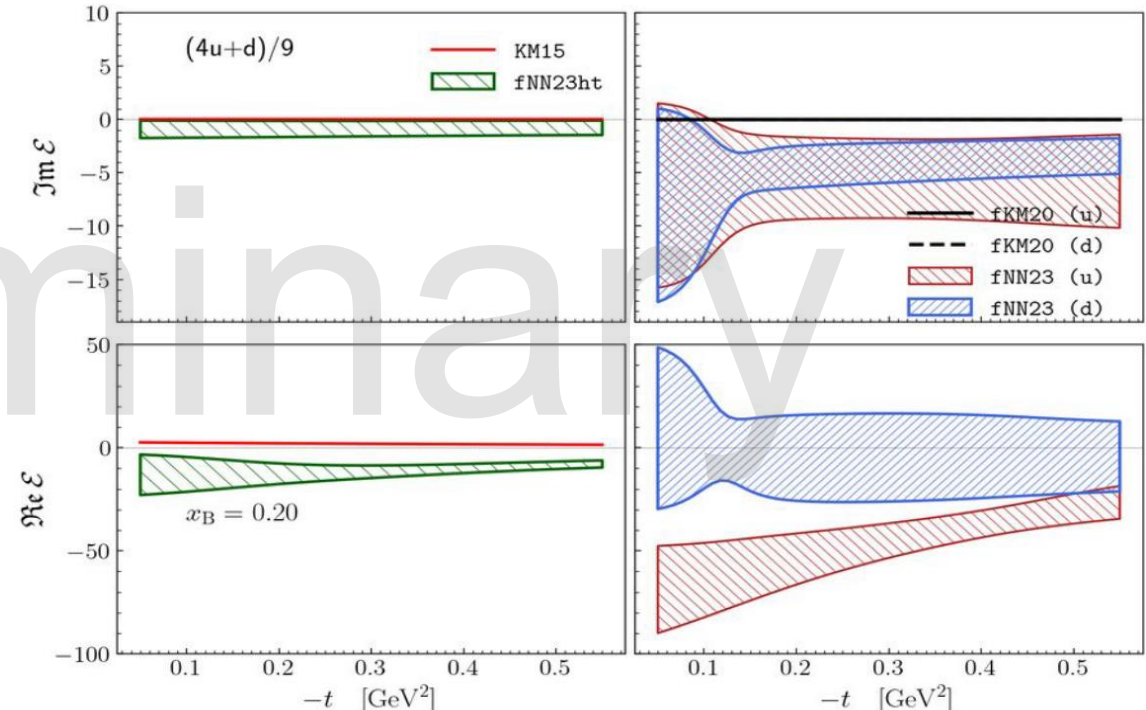


Unlike before, CFF E is now cleanly extracted, with no sign ambiguity in $\text{Re } \varepsilon$

- Flavor separation of CFFs H and E



Flavor separation of ImH is slightly better than before, while ReH is worse



we can now perform flavor separation of CFF E, especially ReE



Conclusions

- GPDs are a powerful tool to explore the structure of the nucleons and nuclei
 - Nucleon tomography, quark angular momentum, distribution of forces in the nucleon
- Exclusive reactions can provide important information on nucleon structure
 - DVCS via the extraction of GPDs
- CLAS12 offers a wide kinematical reach over which the GPDs dependence on different kinematical variables can be scanned
 - Data to add constraints on GPDs in unexplored regions of the phase space
 - Possibilities to measure new observables using different experimental configurations
 - Flavor separation of GPDs
- Promising results from incoherent DVCS on deuteron (n and p channels) from CLAS12 data
 - First BSA measurement from neutron-DVCS with tagged neutron
 - First measurement of BSA for proton-DVCS with deuterium target
 - To be compared to free-proton DVCS BSA measured by CLAS12

G. Christiaens, M. Defurne, D. Sokhan V.Ziegler et al., Phys. Rev. Lett. **130**, 211902



backups

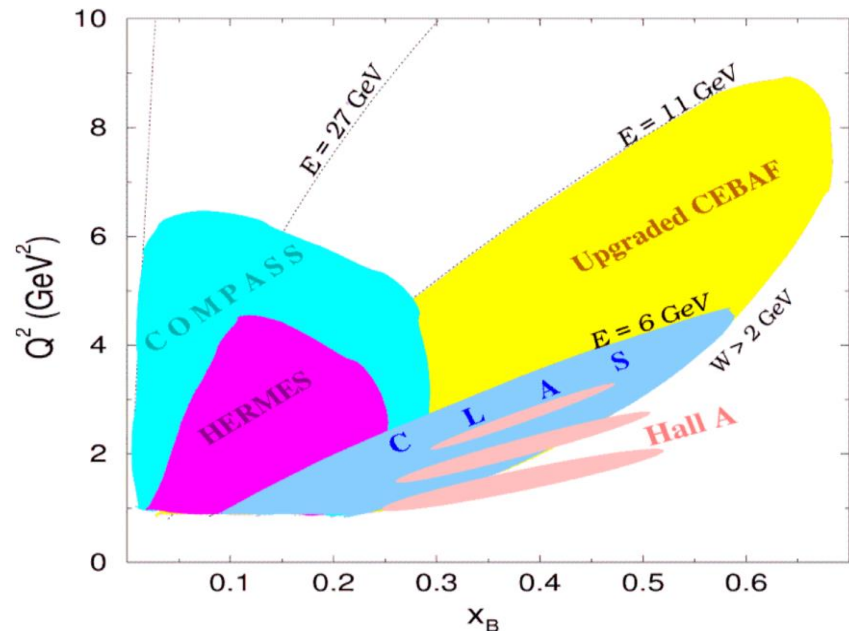
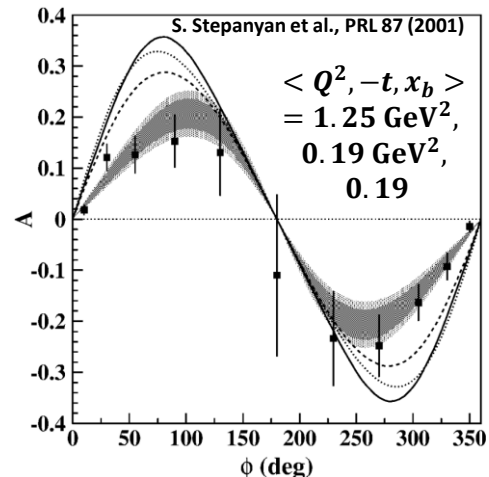


GPD-aimed experiments at JLAB

- **JLAB**

- Hall A:
 - Cross sections
 - Beam-polarised cross section differences
- Hall B (CLAS/CLAS12):
 - Beam and target spin asymmetries
 - Cross section measurements over large phase-space acceptance

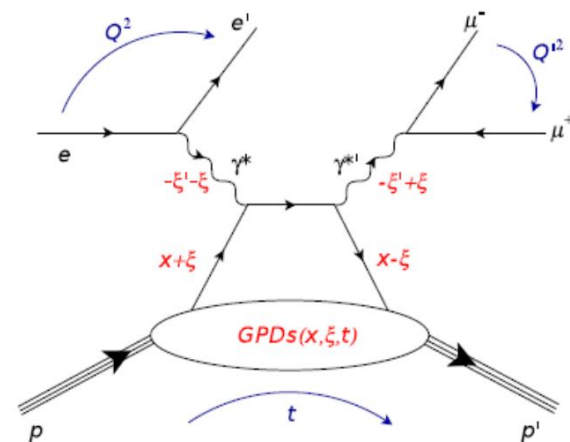
$ep \rightarrow epX$, from CLAS data:
First observation of DVCS-BH
interference





Observable (target)	CFF sensitivity	Status
ITSA(p), IDSA(p)	$\Im\{\mathbf{H}_p, \tilde{\mathbf{H}}_p\}, \Re\{\mathbf{H}_p, \tilde{\mathbf{H}}_p\}$	Data taking ended
ITSA(n), IDSA(n)	$\Im\{\mathbf{H}_n\}, \Re\{\mathbf{H}_n\}$	Data taking ended
tTSA(p)	$\Im\{\mathbf{H}_p\}, \Im\{\mathbf{E}_p\},$	Experiment foreseen for ~2025

- JLab future energy and luminosity upgrades
 - Increase the phase space in which the GPDs are to be scanned
 - And more important: scan x dependence of GPDs: *Double-DVCS*
 - Full kinematics mapping of GPDs: unique direct access to GPDs at $x \neq \pm\xi$
 - Improved detection of muons
- And with a positron beam
 - Study beam charge asymmetries





Decomposition and **abstraction** renders the understanding of a complex system much easier, however, the true nature of the composite system might still be unresolved

In the process of **decomposition** and **abstraction** one usually arrives to the conclusion that most constructing statements of a given theory are **irrational**